



An efficient semi-analytical method for solving fractional differential equations via conformable sense with applications in physics and engineering

Shumoua F. Alrzqi¹, Fatimah A. Alrawajeh², Hany N. Hassan³

¹General Studies Department, Jubail Industrial College, Jubail Industrial City, Saudi Arabia; ²Department of Mathematics, College of Science, Imam Abdulrahman Bin Faisal University, P.O. Box 1982, Dammam, Saudi Arabia; ³Department of Basic Sciences, Deanship of Preparatory Year and Supporting Studies, Imam Abdulrahman Bin Faisal University, P.O. Box 1982, Dammam, Saudi Arabia

Abstract

The aim of the study is to present an efficient semi-analytical technique for solving fractional differential equations (FDEs), the conformable Temimi-Ansari method (CTAM). To evaluate the performance of the method, six nonlinear FDEs are investigated: the Riccati differential equation, the Painlevé equation, the Bernoulli differential equation, the Liénard equation, and the time-fractional Fisher's equation. The accuracy and efficiency of CTAM are assessed through the computation of error norms. To demonstrate the validity and behavior of the obtained solutions, various graphical representations and tables are provided.

Mathematics Subject Classification (2020): 65L05, 34K06, 34K28

Key words and Phrases: conformable fractional derivative; Temimi-Ansari method (TAM); semi-analytical iterative method; fractional differential equations; fractional Fisher's; fractional Riccati; fractional Painlevé; fractional Bernoulli; fractional Liénard.

1. Introduction

In recent years, there has been considerable interest in fractional calculus because of its effectiveness in modeling diverse phenomena observed in numerous scientific and engineering applications.

Email addresses: rizqis@rcjy.edu.sa (Shumoua F. Alrzqi); falrawjih@iau.edu.sa (Fatimah A. Alrawajeh); Hngomaa@iau.edu.sa (Hany N. Hassan)

This growing interest has resulted in significant advances in the development and application of fractional differential equations (FDEs), which have been used to describe a wide range of phenomena in fields such as acoustics, electromagnetics, electrochemistry, engineering, physics, and materials science, including properties that traditional calculus often cannot address [1–8]. Despite their versatility, analytical solutions to FDEs remain difficult to obtain due to their nonlinear terms. As a result, many researchers have developed semi-analytical approach to address these equations, which can produce accurate approximate solutions. Among the most often utilized methods are procedures such as the conformable fractional reduced differential transform (CFRDTM) [9], Homotopy analysis method [10], Picard method [11], conformable reduced differential transform method (CRDTM) [12], B-spline collocation method [13], etc. Among these, the Temimi and Ansari Method (TAM) [14, 15], developed by Temimi and Ansari has demonstrated advantages due to its capability to address differential equations across both linear and nonlinear equations of an integer order. Compared to many other methods, TAM does not depend on additional parameters or limited assumptions whenever addressing nonlinear terms. The purpose of this study is to extend the applicability of the Temimi and Ansari Method (TAM) to nonlinear FDEs by using the conformable fractional operator. This modification enables the development of both approximate and semi-analytical solutions, providing an effective approach to addressing the challenges associated with such equations. To demonstrate the efficiency of the proposed method, we consider several fundamental FDEs. Among them is the Riccati equation, which has been extensively applied in diverse fields such as economics, physics, and epidemiology, highlighting versatility and utility in many scientific subjects [16]. We additionally investigate the Painlevé equations, which have an important role in simulating complex physical phenomena, such as simulations of electric fields in quantum gravity, and random matrix theory [17, 18]. Bernoulli's equation plays a vital role in addressing force and energy-related problems that frequently arise in engineering. It forms the theoretical basis for hydraulic mechanics [19]. The Liénard equations are similarly important since they are used to simulate a wide range of dynamical phenomena that extend to fields such as biology, mechanics, electrical systems, mathematics, and engineering [20]. We additionally investigate Fisher's equation, which is widely utilized to describe the propagation of beneficial genes, as an example of FPDEs. It is essential for simulating phenomena including autocatalytic chemical reactions and Brownian motion [21, 22]. Considering these challenges, the main goal of this study is to provide an efficient semi-analytical technique that can address some of the limitations of current semi-analytical methods by handling significant classes of nonlinear FDEs that appear in physics and engineering. We intend to evaluate the performance of the proposed method in terms of accuracy, convergence, and computational efficiency by comparing it with exact solutions and with results previously reported in the literature.

The article has the following structure: The first section introduces and discusses the motivation for the investigation. The second section explores the definition and the primary properties of the conformable fractional derivative. In the third section, the essential concepts of the conformable Temimi-Ansari Method (CTAM) are presented in terms of FDEs. The fourth section utilizes the presented method on several nonlinear FDEs and investigates the results obtained. Finally, the fifth section concludes with the study results.

2. Definition and Properties of the Conformable Fractional Derivative

Through the years, numerous definitions of fractional calculus have been proposed. Among them, the conformable fractional derivative was discovered as a powerful and practical tool. The conformable derivative preserves numerous fundamental properties of the classical derivative, such as linearity and the product, quotient, chain, and power rules, making it simpler to deal with both linear and nonlinear FDEs. For a wide range of physical models, the use of a conformable derivative is often combined with standard reductions such as travelling-wave transformations, which convert FDEs into nonlinear ODEs of integer order, making it ideal for nonlinear FDEs and the CTAM technique

developed in the current study [23, 24, 25]. This section clarifies the basic concepts and primary properties of conformable calculus, which serve as the theoretical basis for the method proposed in this study [26–28].

Definition 2.1. Let $w:[0,\infty) \rightarrow \mathbb{R}$ be a function. The conformable fractional derivative of ψ of order $\delta \in (0,1]$ at a point $\zeta > 0$ is defined by [27, 26]:

$$(\mathcal{D}_\delta \psi)(\zeta) = \lim_{\varepsilon \rightarrow 0} \frac{\psi(\zeta + \varepsilon \zeta^{1-\delta}) - \psi(\zeta)}{\varepsilon}.$$

Definition 2.2. Let ψ be a function that is differentiable up to order v at a point $\zeta > 0$. For any $\delta \in (v, v+1]$, let $\lceil \delta \rceil$ denote the least integer not smaller than δ . Then the conformable fractional derivative of ψ of order δ is defined by [26]:

$$(\mathcal{D}_\delta \psi)(\zeta) = \lim_{\varepsilon \rightarrow 0} \frac{\psi^{(\lceil \delta \rceil - 1)}(\zeta + \varepsilon \zeta^{\lceil \delta \rceil - \delta}) - \psi^{(\lceil \delta \rceil - 1)}(\zeta)}{\varepsilon}.$$

Lemma 2.3. [26] Suppose ψ and ϕ are both differentiable of order δ at some point $\zeta > 0$, with $\delta \in (0,1]$. Then the following properties are satisfied:

- (1) **Linearity.** $\mathcal{D}_\delta(\beta\psi + \gamma\phi) = \beta\mathcal{D}_\delta\psi + \gamma\mathcal{D}_\delta\phi$, where $\beta, \gamma \in \mathbb{R}$.
- (2) **Power Function Rule.** $\mathcal{D}_\delta(\zeta^p) = p\zeta^{p-\delta}$, for any $p \in \mathbb{R}$.
- (3) **Constant Function Rule.** $\mathcal{D}_\delta(\psi(\zeta)) = 0$, if $\psi(\zeta) = \lambda$ for constant λ .
- (4) **Product Rule.** $\mathcal{D}_\delta(\psi(\zeta)\phi(\zeta)) = \psi(\zeta)\mathcal{D}_\delta\phi(\zeta) + \phi(\zeta)\mathcal{D}_\delta\psi(\zeta)$.

$$(5) \text{ **Quotient Rule.** } \mathcal{D}_\delta\left(\frac{\psi(\zeta)}{\phi(\zeta)}\right) = \frac{\Phi(\zeta)\mathcal{D}_\delta\psi(\zeta) - \psi(\zeta)\mathcal{D}_\delta\phi(\zeta)}{(\phi(\zeta))^2}.$$

- (6) **Higher-Order Derivative.** If ψ is differentiable at ζ , then $\mathcal{D}_\delta\psi(\zeta) = \zeta^{1-\delta} \frac{d}{d\zeta} \psi(\zeta)$.

Lemma 2.4. [26] If ψ is v -times differentiable at $\zeta > 0$, then for any $\delta \in (v, v+1]$, the conformable fractional derivative satisfies:

$$\mathcal{D}_\delta\psi(\zeta) = \zeta^{\lceil \delta \rceil - \delta} \frac{d^{\lceil \delta \rceil}}{d\zeta^{\lceil \delta \rceil}} \psi(\zeta).$$

3. The Proposed Method: Conformable Temimi-Ansari Method (CTAM) for Fractional Differential Equations

The conformable Temimi-Ansari method (CTAM) is a practical semi-analytical approach for nonlinear FDEs, which eliminates the need for Lagrange multipliers and Adomian polynomials, compared to the variational iteration method and the Adomian decomposition method. As a result, the iterative process maintains a very simple mathematical structure while achieving accuracy better than various methods, with a lower processing cost. To clarify the main concept of the technique, the following generic form of a non-homogeneous FDE is considered as follows [15, 29]

$$\mathcal{L}(u(x)) + \mathcal{N}(u(x)) + \mathcal{G}(x) = 0, \quad n-1 < \alpha \leq n,$$

with the boundary conditions

$$\mathcal{B}(u, \frac{du}{dx}) = 0,$$

We start by employing the conformable fractional derivative, which is defined as $\mathcal{L} = T^{\alpha-1} u(x) = T^{1-\alpha} \frac{d}{dt} u(x)$, where $T^{\alpha-1} u(x) := \mathcal{D}_\alpha u(x)$ using Lemma 2.3, property (6) with $\delta = \alpha$, here $u(x)$ is the unknown function, x is the independent variable, and t is the dependent variable. The general linear and nonlinear differential operators are denoted by \mathcal{N} , and the boundary operator by \mathcal{B} . The known continuous functions are expressed as $\mathcal{G}(x)$. In this context, the conformable formulation depends on the generic differential operator \mathcal{L} . When necessary, linear and nonlinear variables can be combined to simulate more complicated systems. A detailed convergence analysis of the method has been presented in [15, 29, 30, 31], verifying its mathematical accuracy.

As a first step in the proposed method, the nonlinear term is isolated, yielding the following initial condition

$$T^{\alpha-1} u_0(x) = \mathcal{G}(x), \quad \mathcal{B}(u_0, \frac{du_0}{dx}) = 0.$$

By substituting the conformable fractional derivative and differentiating the left side with respect to t , the following expression is obtained

$$\frac{d}{dx} u_0(x) = T^{\alpha-1}(\mathcal{G}(x)), \quad \mathcal{B}(u_0, \frac{du_0}{dx}) = 0.$$

The initial solution u_0 is obtained by integrating both sides of the equation with respect to t and solving the equation with the given conditions. The subsequent iteration is then derived by solving the following expression

$$T^{\alpha-1} u_1(x) + \mathcal{N}(u_0(x)) = \mathcal{G}(x), \quad \mathcal{B}(u_1, \frac{du_1}{dx}) = 0.$$

By substituting the conformable fractional derivative and differentiating the left side with respect to t , followed by integrating both sides of the equation with respect to t and applying the conditions, the solution for u_1 is obtained as follows

$$\frac{d}{dx} u_1(x) = T^{\alpha-1}(-\mathcal{N}(u_0(x)) + \mathcal{G}(x)), \quad \mathcal{B}(u_1, \frac{du_1}{dx}) = 0.$$

This process leads to the solution of both linear and nonlinear equations through a straightforward iterative step, represented by $u_{n+1}(x)$.

$$\frac{d}{dx} u_{n+1}(x) = T^{\alpha-1}(-\mathcal{N}(u_n(x)) + \mathcal{G}(x)), \quad \mathcal{B}(u_{n+1}, \frac{du_{n+1}}{dx}) = 0.$$

In the CTAM approach, each $u_{n+1}(x)$ represents an iterative solution to Eq. (1). The iterative method is formulated to be straightforward to implement, with each consecutive approximation improving the accuracy of its predecessor. As iterations increase, the semi-analytical solution converges to the exact solution of Eq. (1). As a result, the method produces a reliable and accurate semi-analytical approximation that is consistent with the exact solution.

$$u(x) = \lim_{n \rightarrow \infty} u_n(x).$$

4. Applications and Discussion

This section presents and discusses the semi-analytical results obtained for several nonlinear FDEs with applications, using the CTAM. The effectiveness and accuracy of the proposed method are assessed by comparing the CTAM solutions with the analytical solutions. To support this evaluation, numerous tables and figures are presented. All symbolic operations and series expansions were performed in Mathematica, while numerical error norms and graphical plots were created in MATLAB.

Example 4.1. The nonlinear fractional Riccati differential equation is considered as [32]:

$$T^\alpha u(x) = 1 - u^2(x), \quad 0 < \alpha \leq 1,$$

given the initial condition

$$u(0) = 0.$$

We start by reformulating Eq. (9) using the semi-analytical iterative approach CTAM, as follows

$$\mathcal{L}(u(x)) = T^\alpha u(x), \quad \mathcal{N}(u(x)) = u^2(x), \quad \mathcal{G}(x) = -1.$$

The first step involves solving the simplified equation

$$\mathcal{L}(u_0(x)) = 1, \quad u_0(0) = 0.$$

Applying the fundamental properties defined in Definition 2.1 yields the following initial approximation

$$u_0(x) = x.$$

Then, the subsequent iteration can be computed using

$$\mathcal{L}(u_1(x)) + \mathcal{N}(u_0(x)) + \mathcal{G}(x) = 0, \quad u_1(0) = 0.$$

By applying the conformable derivative properties 2.1 and integrating both sides of Eq. (14), the next approximation is obtained as

$$u_1(x) = \frac{x^\alpha (\alpha - \alpha x^2 + 2)}{\alpha(\alpha + 2)}.$$

Proceeding to the next iteration, the following equation is used

$$\mathcal{L}(u_2(x)) + \mathcal{N}(u_1(x)) + \mathcal{G}(x) = 0, \quad u_2(0) = 0.$$

Applying the same properties defined in definition 2.1 and integrating both sides of Eq. (16) results in

$$\begin{aligned} u_2(x) = & \frac{1}{3\alpha^3(\alpha + 2)^2(3\alpha + 2)(3\alpha + 4)} \\ & \times \left[-3\alpha^3(3\alpha + 2)x^{3\alpha+4} - (\alpha + 2)^2(9\alpha^2 + 18\alpha + 8)x^{3\alpha} \right. \\ & \left. + 6\alpha^2(3\alpha^2 + 10\alpha + 8)x^{3\alpha+2} + 3\alpha^2(\alpha + 2)^2(9\alpha^2 + 18\alpha + 8)x^\alpha \right]. \end{aligned}$$

As defined in Eq. (8), each iteration of $u_n(x)$ provides an approximation to the solution of Eq. (9). With each iteration, the semi-analytical solution gets closer to the exact solution. The series solution obtained by CTAM is expressed as

$$u(x) = \lim_{n \rightarrow \infty} u_n(x) \simeq u_8(x).$$

This series solution converges to the exact solution when $\alpha = 1$, given by [32]

$$u(x) = \frac{e^{2x} - 1}{e^{2x} + 1}.$$

Figure 1(A), presents the results obtained from the proposed CTAM method using the 8-th iteration for various values α , along with the exact solution for $\alpha = 1$, demonstrating that the solutions closely match the exact solution as α approaches 1, exhibit significant consistency across various fractional orders. When $\alpha = 1$, 1(B) shows the absolute error between the CTAM solution at the 8-th iteration and the exact solution. Table 1 provides a thorough results comparison between the exact, Picard method, and CTAM solutions for $\alpha = 1$, highlighting the decreased error and closer approximation to the exact solution with lower error compared to the results in [32]. Those findings indicate that increasing the number of iterations enhances the accuracy of the technique's solution, which makes it closer to the exact solution.

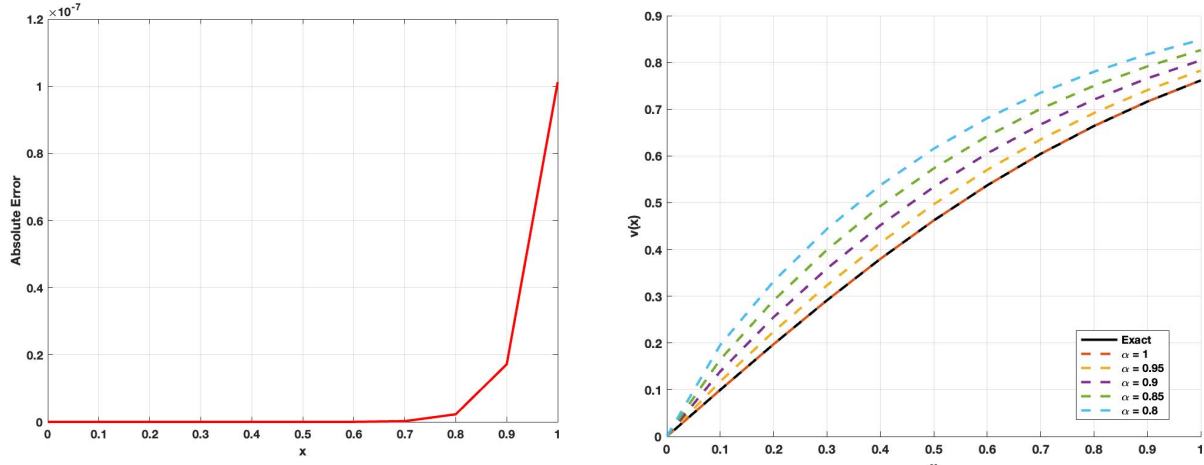


Figure 1: (A) The results of the proposed method in Example 4.1 with 8-th iteration for different α values and exact solution at $\alpha = 1$. (B) The absolute errors between the proposed method and the exact solution for $\alpha = 1$.

Table 1: A comparison between the 8-th CTAM solution, previous studies, and the exact solution at $\alpha = 1$ of Example 4.1.

x	u_{Exact}	u_{CTAM}	E_{CTAM}	E_{Picard} [32]
0	0	0	0	0
0.1	0.0996680	0.0996671	1.3878×10^{-20}	8.689×10^{-14}
0.2	0.1973753	0.1973753	2.7756×10^{-20}	2.426×10^{-13}
0.3	0.2913126	0.2913126	5.5511×10^{-20}	6.055×10^{-13}
0.4	0.3799490	0.3799481	8.4377×10^{-15}	1.437×10^{-12}
0.5	0.4621172	0.4621172	5.1092×10^{-13}	2.776×10^{-12}
0.6	0.5370496	0.5370496	1.3955×10^{-11}	7.13×10^{-12}
0.7	0.6043678	0.6043678	2.1831×10^{-13}	2.622×10^{-10}
0.8	0.6640368	0.6640368	2.2667×10^{-12}	3.525×10^{-09}
0.9	0.7162979	0.7162979	1.7160×10^{-11}	7.782×10^{-08}
1	0.7615942	0.7615943	1.0121×10^{-7}	1.381×10^{-05}

Example 4.2. The nonlinear fractional Riccati differential equation is considered as [32]:

$$T^\alpha u(x) = 1 + 2u(x) - u^2(x), \quad 0 < \alpha \leq 1,$$

with the initial condition

$$u(0) = 0.$$

To demonstrate the adaptability of the proposed method, Eq. (20) is reformulated within the CTAM as follows

$$\mathcal{L}(u(x)) = T^\alpha u(x), \quad \mathcal{N}(u(x)) = -2u(x) + u^2(x), \quad \mathcal{G}(x) = -1.$$

The initial issue that needs to be solved is given by

$$\mathcal{L}(u_0(x)) = 1, \quad u_0(0) = 0.$$

Based on the properties outlined in definition 2.1, we get the following initial approximation

$$u_0(x) = x.$$

The next iteration is calculated using

$$\mathcal{L}(u_1(x)) + \mathcal{N}(u_0(x)) + \mathcal{G}(x) = 0, \quad u_1(0) = 0.$$

Which, after integration and simplification both sides of Eq. (25), leads to

$$u_1(x) = -\frac{x^\alpha (\alpha^2(x^2 - 2x - 1) + \alpha(x^2 - 4x - 3) - 2)}{\alpha(\alpha+1)(\alpha+2)}.$$

Continuing the iterative process yields the next approximation by solving

$$\mathcal{L}(u_2(x)) + \mathcal{N}(u_1(x)) + \mathcal{G}(x) = 0, \quad u_2(0) = 0.$$

By applying the properties of the conformable derivative defined in definition 2.1, followed by integrating both sides of Eq. (27), we get

$$\begin{aligned} u_2(x) = & -\frac{x^\alpha}{3\alpha^3(2\alpha+1)(3\alpha+1)(3\alpha+2)(3\alpha+4)(\alpha^2+3\alpha+2)^2} \\ & \times \left[-3\alpha^2(\alpha^2+3\alpha+2)^2(54\alpha^4+153\alpha^3+147\alpha^2+58\alpha+8) \right. \\ & + 3\alpha^3(\alpha+1)^2(18\alpha^3+27\alpha^2+13\alpha+2)x^{2\alpha+4} \\ & + (\alpha^2+3\alpha+2)^2(54\alpha^4+153\alpha^3+147\alpha^2+58\alpha+8)x^{2\alpha} \\ & - 12\alpha^3(\alpha+2)^2(27\alpha^4+90\alpha^3+105\alpha^2+50\alpha+8)x^{\alpha+1} \\ & + 12\alpha^2(\alpha+2)^2(18\alpha^4+63\alpha^3+79\alpha^2+42\alpha+8)x^{2\alpha+1} \\ & - 4\alpha^3(54\alpha^5+261\alpha^4+453\alpha^3+352\alpha^2+124\alpha+16)x^{2\alpha+3} \\ & + 3\alpha^3(54\alpha^6+315\alpha^5+714\alpha^4+805\alpha^3+476\alpha^2+140\alpha+16)x^{\alpha+2} \\ & + 6\alpha^2(18\alpha^6+111\alpha^5+233\alpha^4+177\alpha^3+7\alpha^2-34\alpha-8)x^{2\alpha+2} \\ & \left. - 3\alpha(\alpha^2+3\alpha+2)^2(54\alpha^4+153\alpha^3+147\alpha^2+58\alpha+8)x^\alpha \right]. \end{aligned}$$

Following this process, as defined in Eq. (8), each iteration $u_n(x)$ is an approximate solution to Eq. (20). Then, the semi-analytical series solution using CTAM is expressed as follows

$$u(x) = \lim_{n \rightarrow \infty} u_n(x) \simeq u_7(x).$$

The solution reaches the exact solution when $\alpha = 1$, given by [32]

$$u(x) = 1 + \sqrt{2} \tanh \left(\sqrt{2}t + \frac{1}{2} \log \left(\frac{\sqrt{2}-1}{\sqrt{2}+1} \right) \right).$$

Figure 2 (A) illustrates the comparison between the exact solution and the 7-th iteration obtained using the CTAM method for Eq. (20) across various α values at $x = 1$, Figure 2 (B) displays the absolute error between 7-th CTAM iteration and the exact solution. The accuracy of the 3-rd and 7-th iterations are highlighted in Table 2, the results show that, for the same number of iterations, CTAM produces smaller errors than Picard's method in [32] and a more accurate approximation of the exact solution, demonstrating significant convergence. Moreover, the effectiveness of the method improves as the number of iterations increases, with the absolute error decreasing from 10^{-4} to as low as 10^{-7} . showing that the CTAM approach effectively solves FDEs with high accuracy and fast convergence.

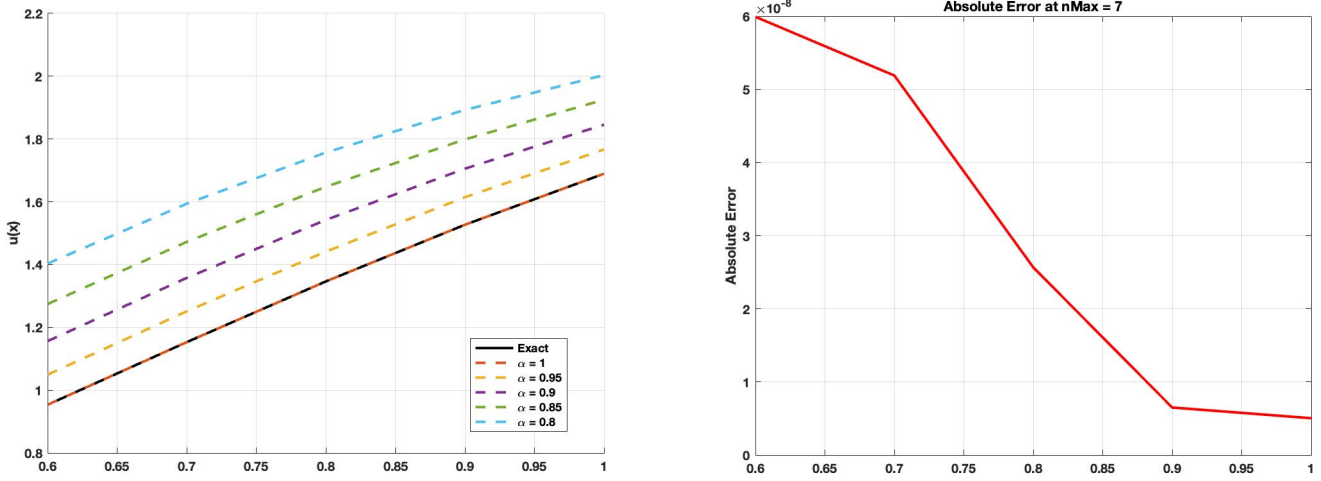


Figure 2: (A) The results of the proposed method in Example 4.2 with 7-th iteration for different α values and exact solution at $\alpha = 1$. (B) The absolute errors between the proposed method and the exact solution for $\alpha = 1$.

Table 2: A comparison between the 3-rd, and the 7-th CTAM solution, previous studies, and the exact solution at $\alpha = 1$ of Example 4.2.

x	u_{Exact}	u_{CTAM} (Proposed method)	E_{CTAM} (3 iterations)	E_{CTAM} (7 iterations)	E_{Picard} (3 iterations) [32]	E_{Picard} (7 iterations) [32]
0.6	0.953566	0.953566	9.7760×10^{-4}	0.5993×10^{-7}	4.25×10^{-4}	3×10^{-7}
0.7	1.152949	1.152949	8.9484×10^{-4}	5.1903×10^{-7}	5.59×10^{-4}	4.15×10^{-7}
0.8	1.346364	1.346364	5.7367×10^{-4}	2.5666×10^{-7}	7.2152×10^{-5}	2.76×10^{-7}
0.9	1.526911	1.526911	4.0568×10^{-4}	6.5035×10^{-7}	3.33527×10^{-3}	1.06×10^{-5}
1	1.689498	1.689498	8.4708×10^{-4}	5.0411×10^{-7}	1.3963×10^{-2}	8.33×10^{-5}

Example 4.3. The nonlinear higher order fractional Painlevé differential equation is considered as [33]:

$$T^\alpha u(x) = 6u^2(x) + x, \quad 1 < \alpha \leq 2,$$

and the initial conditions

$$u_0(0) = 0, \quad ((u_0))_x(0) = 1.$$

Eq. (31) is reformulated using the CTAM as follows

$$\mathcal{L}(u(x)) = T^\alpha u''(x), \quad \mathcal{N}(u(x)) = -6u^2(x), \quad \mathcal{G}(x) = -x.$$

The initial issue to be addressed is defined by

$$\mathcal{L}(u_0(x)) = x, \quad u_0(0) = 0, \quad ((u_0))_x(0) = 1.$$

Applying the fundamental properties outlined in definition 2.1, leads to the first iteration

$$u_0(x) = \frac{x(\alpha^2 + \alpha + x^\alpha)}{\alpha(\alpha + 1)}.$$

The next iteration is obtained from

$$\mathcal{L}(u_1(x)) + \mathcal{N}(u_0(x)) + \mathcal{G}(x) = 0, \quad u_1(0) = 0, \quad ((u_1))_x(0) = 1.$$

This yields the following expression after integrating Eq. (36)

$$\begin{aligned} u_1(x) = & \frac{x}{\alpha^2(\alpha+1)^2(\alpha+2)(2\alpha+1)(3\alpha+1)(3\alpha+2)} \\ & \times \left[\alpha^2(\alpha+1)^2(18\alpha^4 + 63\alpha^3 + 67\alpha^2 + 28\alpha + 4) + 6(2\alpha^2 + 5\alpha + 2)x^{3\alpha+1} \right. \\ & + 6\alpha(9\alpha^3 + 27\alpha^2 + 20\alpha + 4)x^{2\alpha+1} + 6\alpha^2(18\alpha^4 + 45\alpha^3 + 40\alpha^2 + 15\alpha + 2)x^{\alpha+1} \\ & \left. + \alpha(18\alpha^5 + 81\alpha^4 + 130\alpha^3 + 95\alpha^2 + 32\alpha + 4)x^\alpha \right]. \end{aligned}$$

This process is continued, with the third iteration derived from

$$\mathcal{L}(u_2(x)) + \mathcal{N}(u_1(x)) + \mathcal{G}(x) = 0, \quad u_2(0) = 0, \quad ((u_2))_x(0) = 1.$$

By integrating both sides of Eq. (38) and applying the fundamental properties of definition 2.1, the third approximation is obtained as

$$u_2(x)$$

$$\begin{aligned} &= \frac{x}{\alpha^4(\alpha+1)^4(\alpha+2)^2(2\alpha+3)(3\alpha+4)(4\alpha+3)(5\alpha+2)(5\alpha+3)(5\alpha+4)(7\alpha+3)(7\alpha+4)(18\alpha^3 + 27\alpha^2 + 13\alpha + 2)^2} \\ &\times \left[\alpha^3(\alpha+1)^3(18\alpha^4 + 63\alpha^3 + 67\alpha^2 + 28\alpha + 4)^2(147000\alpha^8 + 938350\alpha^7 + 2534755\alpha^6 + 3789224\alpha^5 \right. \\ &+ 3434825\alpha^4 + 1936782\alpha^3 + 664488\alpha^2 + 127008\alpha + 10368)x^\alpha + 6\alpha^4(\alpha+1)^3(18\alpha^3 + 27\alpha^2 + 13\alpha + 2)^2 \\ &(147000\alpha^9 + 1232350\alpha^8 + 4411455\alpha^7 + 8858734\alpha^6 + 11013273\alpha^5 + 8806432\alpha^4 + 4538052\alpha^3 + 1455984\alpha^2 \\ &+ 264384\alpha + 20736)x^{\alpha+1} + 6\alpha^3(9\alpha^4 + 36\alpha^3 + 47\alpha^2 + 24\alpha + 4)^2(294000\alpha^9 + 2023700\alpha^8 + 6007860\alpha^7 \\ &+ 10113203\alpha^6 + 10658874\alpha^5 + 7308389\alpha^4 + 3265758\alpha^3 + 918504\alpha^2 + 147744\alpha + 10368)x^{2\alpha+1} + 36\alpha^4(18\alpha^4 \\ &+ 45\alpha^3 + 40\alpha^2 + 15\alpha + 2)^2(73500\alpha^8 + 505925\alpha^7 + 1446840\alpha^6 + 2259107\alpha^5 + 2117976\alpha^4 + 1226252\alpha^3 \\ &+ 429648\alpha^2 + 83520\alpha + 6912)x^{2\alpha+2} + 6\alpha^2(2\alpha^3 + 7\alpha^2 + 7\alpha + 2)^2(1323000\alpha^{10} + 9768150\alpha^9 + 31551945\alpha^8 \\ &+ 58792511\alpha^7 + 70085951\alpha^6 + 55922911\alpha^5 + 30281080\alpha^4 + 10997028\alpha^3 + 2565360\alpha^2 + 347328\alpha \\ &+ 20736)x^{3\alpha+1} + 72\alpha^3(3\alpha^2 + 4\alpha + 1)^2(882000\alpha^{11} + 8423100\alpha^{10} + 35389180\alpha^9 + 86497289\alpha^8 + 136913686\alpha^7 \\ &+ 147648971\alpha^6 + 110899882\alpha^5 + 58115132\alpha^4 + 20854296\alpha^3 + 4887072\alpha^2 + 673920\alpha + 41472)x^{3\alpha+2} \\ &+ 72\alpha^4(18\alpha^3 + 27\alpha^2 + 13\alpha + 2)^2(49000\alpha^8 + 296450\alpha^7 + 762435\alpha^6 + 1091413\alpha^5 + 952799\alpha^4 + 520137\alpha^3 \\ &+ 173574\alpha^2 + 32400\alpha + 2592)x^{3\alpha+3} + 36\alpha^2(\alpha+2)^2(3638250\alpha^{12} + 31740975\alpha^{11} + 124090230\alpha^{10} \\ &+ 287658229 + 440695538\alpha^8 + 470396445\alpha^7 + 358949074\alpha^6 + 197421611\alpha^5 + 77717676\alpha^4 \\ &+ 21367380\alpha^3 + 3896496\alpha^2 + 423360\alpha + 20736)x^{4\alpha+2} + 108\alpha^3(9\alpha^2 + 9\alpha + 2)^2(73500\alpha^9 + 597800\alpha^8 \\ &+ 2065465\alpha^7 + 3983132\alpha^6 + 4733971\alpha^5 + 3606056\alpha^4 + 1766092\alpha^3 + 537936\alpha^2 + 92736\alpha + 6912)x^{4\alpha+3} \\ &+ 72\alpha(2\alpha^2 + 5\alpha + 2)^2(52920\alpha^9 + 390726\alpha^8 + 1249377\alpha^7 + 2270627\alpha^6 + 2584661\alpha^5 + 1910743\alpha^4 \\ &+ 917098\alpha^3 + 275448\alpha^2 + 46944\alpha + 3456)x^{5\alpha+2} + 216\alpha^2(899640\alpha^{12} + 9457686\alpha^{11} + 44007357\alpha^{10} \\ &+ 119825845\alpha^9 + 212683647\alpha^8 + 259401895\alpha^7 + 223138872\alpha^6 + 136565998\alpha^5 + 59098188\alpha^4 \\ &+ 17659608\alpha^3 + 3463632\alpha^2 + 400896\alpha + 20736)x^{5\alpha+3} + 72\alpha(\alpha+2)^2(441000\alpha^9 + 2962050\alpha^8 + 8542615\alpha^7 \\ &+ 13902427\alpha^6 + 14093699\alpha^5 + 9245171\alpha^4 + 3930246\alpha^3 + 1045512\alpha^2 + 158112\alpha + 10368)x^{6\alpha+3} \\ &+ 216(2\alpha^2 + 5\alpha + 2)^2(3000\alpha^6 + 16150\alpha^5 + 34845\alpha^4 + 38531\alpha^3 + 23034\alpha^2 + 7056\alpha + 864)x^{7\alpha+3} + \alpha^4(\alpha+1)^4 \\ &(18\alpha^4 + 63\alpha^3 + 67\alpha^2 + 28\alpha + 4)^2(147000\alpha^8 + 938350\alpha^7 + 2534755\alpha^6 + 3789224\alpha^5 + 3434825\alpha^4 \\ &+ 1936782\alpha^3 + 664488\alpha^2 + 127008\alpha + 10368) \left. \right]. \end{aligned}$$

As described in Eq. (8), each function $u_n(x)$ provides an increasingly accurate approximation to the solution of Eq. (31). The semi-analytical solution is therefore represented as

$$u(x) = \lim_{n \rightarrow \infty} u_n(x) \simeq u_5(x).$$

The semi-analytical results demonstrate that the solution to Eq. (31) closely matches the exact solution when $\alpha = 2$. Figure 3 (A) displays the CTAM solutions at the 5-th iteration for many values of α , compared with the exact solution for $\alpha = 2$. The CTAM results demonstrate the method's accuracy over fractional orders, closely matching the analytical solution. The absolute error corresponding to $\alpha = 2$, shown in Figure 3 (B) remains extremely low across the interval, which reflects strong convergence characteristics. Table 3 provides a detailed comparison of the CTAM solution at $\alpha = 2$ with the exact solution, along with additional results for $\alpha = 1.9$, $\alpha = 1.8$, and $\alpha = 1.7$. The CTAM approximations remain close to the exact solution, even for lower fractional orders, the method maintains robust accuracy. These findings confirm the capability of CTAM, with high precision and minimal computational cost.

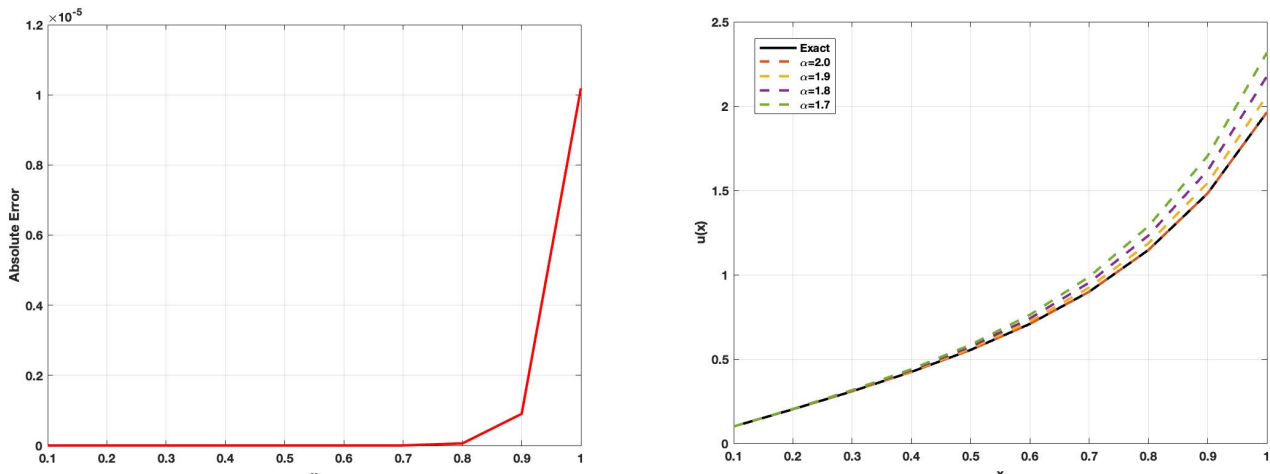


Figure 3: (A) The results of the proposed method in Example 4.3 with 5-th iteration for different α values and exact solution at $\alpha = 2$. (B) The absolute errors between the proposed method and the exact solution for $\alpha = 2$.

Table 3: A comparison between the 5-th CTAM solution and the exact solution at $\alpha = 2$ of Example 4.3.

x	u_{Exact}	$u_{CTAM} \alpha = 2$	E_{CTAM}	$u_{CTAM} \alpha = 1.9$	$u_{CTAM} \alpha = 1.8$	$u_{CTAM} \alpha = 1.7$
0.1	0.100217	0.100217	0	0.100295	0.100404	0.100555
0.2	0.202139	0.202139	2.200×10^{-14}	0.202712	0.203451	0.204408
0.3	0.308631	0.308631	2.7400×10^{-13}	0.310493	0.312804	0.315687
0.4	0.423986	0.423986	1.4860×10^{-12}	0.428337	0.433605	0.440025
0.5	0.554340	0.554340	5.2260×10^{-11}	0.562855	0.573003	0.585185
0.6	0.708462	0.708462	3.1116×10^{-10}	0.723461	0.741164	0.762230
0.7	0.899250	0.899250	1.5184×10^{-9}	0.924034	0.953140	0.987648
0.8	1.146532	1.146532	6.0144×10^{-8}	1.186023	1.232370	1.287349
0.9	1.482524	1.482523	8.9931×10^{-7}	1.544535	1.617538	1.704545
1.0	1.963128	1.963117	1.0186×10^{-5}	2.060956	2.176951	2.316416

Example 4.4. The nonlinear fractional Bernoulli differential equation is considered as [34]:

$$6D_x^\alpha u - 2u = xu^4, \quad 0 < \alpha \leq 1,$$

and the initial condition

$$u(0) = -2.$$

By reformulating Eq. (41) using the semi-analytical iterative method CTAM, yields the following

$$\mathcal{L}(u(x)) = 6D_x^\alpha u, \mathcal{N}(u(x)) = -2u - xu^4, \mathcal{G}(x) = 0.$$

The primary issue to address is

$$\mathcal{L}(u_0(x)) = 0, u_0(0) = -2.$$

Which leads to the first iteration, based on the properties of definition 2.1, as

$$u_0(x) = -2$$

The next approximation is computed from

$$\mathcal{L}(u_1(x)) + \mathcal{N}(u_0(x)) + \mathcal{G}(x) = 0, u_1(0) = -2.$$

Using conformable derivative properties 2.1, we can integrate both sides of Eq. (46) and get

$$u_1(x) = -\frac{2(3\alpha^2 + 3\alpha - 4\alpha x^{\alpha+1} + \alpha x^\alpha + x^\alpha)}{3\alpha(\alpha+1)}$$

Continuing the iterative process, the next approximation is derived from

$$\mathcal{L}(u_2(x)) + \mathcal{N}(u_1(x)) + \mathcal{G}(x) = 0, u_2(0) = -2.$$

Which results, after integration Eq. (48) and simplification, in the expression

$$\begin{aligned} u_2(x) = & \frac{1}{1215\alpha^4(\alpha+1)^5(2\alpha+1)(3\alpha+1)(3\alpha+2)} \\ & \times \frac{1}{(4\alpha+1)(4\alpha+3)(5\alpha+1)(5\alpha+2)(5\alpha+3)(5\alpha+4)} \\ & \times \left[-810\alpha^3(\alpha+1)^5(180000\alpha^9 + 810000\alpha^8 + 1585750\alpha^7 + 1770125\alpha^6 + 1239787\alpha^5 \right. \\ & + 564155\alpha^4 + 166531\alpha^3 + 30704\alpha^2 + 3204\alpha + 144)x^\alpha - 135\alpha^2(\alpha+1)^5(180000\alpha^9 \\ & + 810000\alpha^8 + 1585750\alpha^7 + 1770125\alpha^6 + 1239787\alpha^5 + 564155\alpha^4 + 166531\alpha^3 + 30704\alpha^2 \\ & + 3204\alpha + 144)x^{2\alpha} + 3240\alpha^4(\alpha+1)^4(180000\alpha^9 + 810000\alpha^8 + 1585750\alpha^7 + 1770125\alpha^6 \\ & + 1239787\alpha^5 + 564155\alpha^4 + 166531\alpha^3 + 30704\alpha^2 + 3204\alpha + 144)x^{\alpha+1} \\ & + 1080\alpha^3(\alpha+1)^4(5\alpha+4)^2(18000\alpha^7 + 57600\alpha^6 + 76495\alpha^5 + 54529\alpha^4 + 22493\alpha^3 \\ & + 5363\alpha^2 + 684\alpha + 36)x^{2\alpha+1} - 8640\alpha^4(\alpha+1)^3(180000\alpha^9 + 810000\alpha^8 + 1585750\alpha^7 \\ & + 1770125\alpha^6 + 1239787\alpha^5 + 564155\alpha^4 + 166531\alpha^3 + 30704\alpha^2 + 3204\alpha + 144)x^{2\alpha+2} \\ & + 2160\alpha^2(\alpha+1)^5(60000\alpha^8 + 250000\alpha^7 + 445250\alpha^6 + 441625\alpha^5 + 266054\alpha^4 \\ & + 99367\alpha^3 + 22388\alpha^2 + 2772\alpha + 144)x^{3\alpha+1} - 17280\alpha^3(\alpha+1)^4(60000\alpha^8 + 230000\alpha^7 \\ & + 375250\alpha^6 + 339875\alpha^5 + 186679\alpha^4 + 63599\alpha^3 + 13111\alpha^2 + 1494\alpha + 72)x^{3\alpha+2} \\ & + 11520\alpha^4(\alpha+1)^2(180000\alpha^9 + 810000\alpha^8 + 1585750\alpha^7 + 1770125\alpha^6 + 1239787\alpha^5 \\ & + 564155\alpha^4 + 166531\alpha^3 + 30704\alpha^2 + 3204\alpha + 144)x^{3\alpha+3} + 480\alpha(\alpha+1)^5(45000\alpha^8 \\ & + 191250\alpha^7 + 348625\alpha^6 + 355375\alpha^5 + 221103\alpha^4 + 85763\alpha^3 + 20192\alpha^2 + 2628\alpha \\ & + 144)x^{4\alpha+1} - 2880\alpha^2(\alpha+1)^4(90000\alpha^8 + 360000\alpha^7 + 612875\alpha^6 + 578625\alpha^5 \\ & + 330581\alpha^4 + 116787\alpha^3 + 24872\alpha^2 + 2916\alpha + 144)x^{4\alpha+2} \\ & + 23040\alpha^3(\alpha+1)^3(45000\alpha^8 + 168750\alpha^7 + 269875\alpha^6 + 240125\alpha^5 + 129853\alpha^4 \\ & + 43649\alpha^3 + 8896\alpha^2 + 1004\alpha + 48)x^{4\alpha+3} - 7680\alpha^4(180000\alpha^{10} + 990000\alpha^9 \right] \end{aligned}$$

$$\begin{aligned}
& + 2395750\alpha^8 + 3355875\alpha^7 + 3009912\alpha^6 + 1803942\alpha^5 + 730686\alpha^4 + 197235\alpha^3 \\
& + 33908\alpha^2 + 3348\alpha + 144)x^{4\alpha+4} + 40(\alpha+1)^5(36000\alpha^8 + 154800\alpha^7 \\
& + 286190\alpha^6 + 296787\alpha^5 + 188600\alpha^4 + 75111\alpha^3 + 18284\alpha^2 + 2484\alpha \\
& + 144)x^{5\alpha+1} - 640\alpha(\alpha+1)^4(36000\alpha^8 + 147600\alpha^7 + 258110\alpha^6 + 250781\alpha^5 \\
& + 147645\alpha^4 + 53773\alpha^3 + 11797\alpha^2 + 1422\alpha + 72)x^{5\alpha+2} \\
& + 3840\alpha^2(\alpha+1)^3(36000\alpha^8 + 140400\alpha^7 + 232910\alpha^6 + 214279\alpha^5 + 119390\alpha^4 \\
& + 41197\alpha^3 + 8588\alpha^2 + 988\alpha + 48)x^{5\alpha+3} - 10240\alpha^3(\alpha+1)^2(36000\alpha^8 + 133200\alpha^7 \\
& + 210590\alpha^6 + 185553\alpha^5 + 99515\alpha^4 + 33219\alpha^3 + 6731\alpha^2 + 756\alpha + 36)x^{5\alpha+4} \\
& + 2048\alpha^4(180000\alpha^9 + 810000\alpha^8 + 1585750\alpha^7 + 1770125\alpha^6 \\
& + 1239787\alpha^5 + 564155\alpha^4 + 166531\alpha^3 + 30704\alpha^2 + 3204\alpha \\
& + 144)x^{5\alpha+5} - 2430\alpha^4(\alpha+1)^5(180000\alpha^9 + 810000\alpha^8 + 1585750\alpha^7 + 1770125\alpha^6 \\
& + 1239787\alpha^5 + 564155\alpha^4 + 166531\alpha^3 + 30704\alpha^2 + 3204\alpha + 144) \Big].
\end{aligned}$$

As outlined in Eq. (8), each iteration $u_n(x)$ represents an approximation to the exact solution of Eq. (41). As more iterations are performed, the CTAM approximation converges progressively toward the exact solution. The approximate series solution can be written as

$$u(x) = \lim_{n \rightarrow \infty} u_n(x) \approx u_4(x).$$

The exact solution when $\alpha = 1$, as reported in (34), is

$$u(x) = -\frac{2}{(4x - 4 + 5 \exp(-x))^{\frac{1}{3}}}.$$

For $\alpha = 1$, the exact solution of Eq. (41) corresponds to the CTAM solution. As illustrated in Figure 4 (A), CTAM solution curve behavior for different values of α , showing strong agreement with the exact solution for $\alpha = 1$. Figure 4 (B) presents the absolute error between the 4-th CTAM iteration and the exact solution for $\alpha = 1$, which remains relatively small across the domain. Table 4 presents a detailed comparison at specific values of x between the CTAM results and the exact solution, confirming the method's high precision at $\alpha = 1$. Moreover, comparisons for $\alpha = 0.9$, $\alpha = 0.8$, and $\alpha = 0.7$ demonstrate that the approach can produce accurate solutions for a variety of fractional orders.

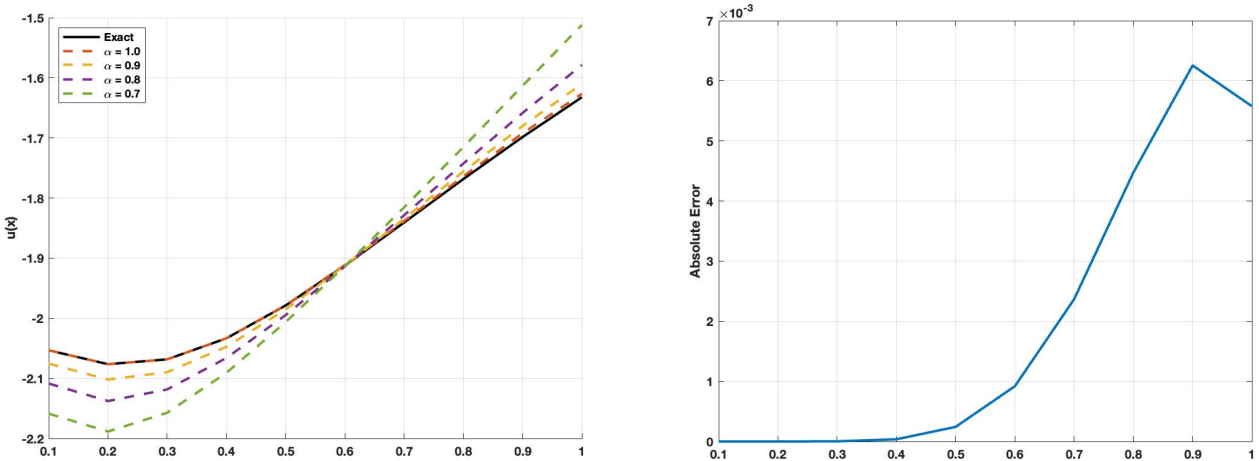


Figure 4: (A) The results of the proposed method in Example 4.4 with 4-th iteration for different α values and exact solution at $\alpha = 1$. (B) The absolute errors between the proposed method and the exact solution for $\alpha = 1$.

Table 4: A comparison between the 4-th CTAM solution and the exact solution at $\alpha=1$ of Example 4.4.

x	u_{Exact}	$u_{CTAM}(\alpha=1)$	E_{CTAM}	$u_{CTAM}(\alpha=0.9)$	$u_{CTAM}(\alpha=0.8)$	$u_{CTAM}(\alpha=0.7)$
0.1	-2.05325724	-2.05325724	2.3100×10^{-13}	-2.075483	-2.108488	-2.158698
0.2	-2.07638030	-2.07638027	2.4829×10^{-8}	-2.101997	-2.137744	-2.188443
0.3	-2.06835905	-2.06835670	2.3466×10^{-6}	-2.089671	-2.118381	-2.157239
0.4	-2.03334848	-2.03331138	3.7107×10^{-5}	-2.047393	-2.066154	-2.090755
0.5	-1.97869330	-1.97845045	2.4286×10^{-4}	-1.985344	-1.994714	-2.006262
0.6	-1.91226155	-1.91134176	9.1978×10^{-4}	-1.912262	-1.913599	-1.913125
0.7	-1.84061406	-1.83824633	2.3677×10^{-3}	-1.834363	-1.828446	-1.815455
0.8	-1.76838175	-1.76390656	4.4752×10^{-3}	-1.755858	-1.742548	-1.715025
0.9	-1.69843155	-1.69217576	6.2558×10^{-3}	-1.680033	-1.658409	-1.613213
1.0	-1.63231819	-1.62674042	5.5778×10^{-3}	-1.610121	-1.578726	-1.511991

Example 4.5. The nonlinear higher degree fractional Liénard equation is considered as [35, 36]:

$$D^\beta u(t) + 0.5D'u + 25u + 25u^3 = 0, \quad 1 < \beta \leq 2,$$

with the initial conditions

$$u(0) = 0.1, \quad u'(0) = 0.$$

Eq. (52) is reformulated using CTAM as follows

$$\mathcal{L}(u(x)) = D^\beta u(t), \quad \mathcal{N}(u(x)) = 0.5D'u + 25u + 25u^3, \quad \mathcal{G}(x) = 0.$$

The initial iteration to solve defined as

$$\mathcal{L}(u_0(x)) = 0, \quad u_0(0) = 0.1, \quad (u_0)_x(0) = 0.$$

Which lead to the first approximation based on the conformable derivative definition 2.1

$$u_0(x) = \frac{1}{10}.$$

Then, we obtain the next iteration from

$$\mathcal{L}(u_1(x)) + \mathcal{N}(u_0(x)) + \mathcal{G}(x) = 0, \quad u_1(0) = 0.1, \quad (u_1)_x(0) = 0.$$

And by integrating both sides of Eq. (57), results in

$$u_1(x) = 0.1 - \frac{2.525t^\alpha}{\alpha(\alpha-1)}.$$

Continuing this process, the following iteration is defined by

$$\mathcal{L}(u_2(x)) + \mathcal{N}(u_1(x)) + \mathcal{G}(x) = 0, \quad u_2(0) = 0.1, \quad (u_2)_x(0) = 0.$$

After applying integration of both sides of Eq. (59) and the fundamental conformable derivative properties 2.1, yields

$$u_2(x) = \frac{1}{t(-1+\alpha)^3 \alpha^4 \left(-\frac{1}{48} + \alpha \left(\frac{1}{4} + \alpha \left(-\frac{55}{48} + \alpha \left(\frac{5}{2} + \left(-\frac{727143689835869}{281474976710659} + \alpha \right) \alpha \right) \right) \right) \right)} \\ \times \left[-\frac{2124264786520 t^{1+3\alpha} \alpha^6}{399822408599} + t^{1+4\alpha} \left(\frac{1030301}{491520} + \alpha \left(-\frac{1030301}{61440} + \alpha \left(\frac{23696923}{491520} + \alpha \left(-\frac{7212107}{122880} + \frac{1030301\alpha}{40960} \right) \right) \right) \right]$$

$$\begin{aligned}
& +t^{2\alpha} \alpha^4 \left(-\frac{510577813299}{38824134714221} + \alpha \left(\frac{1111}{7680} + \alpha \left(-\frac{10411000725475}{17592186044367} + \alpha \left(\frac{4916305898044}{4398046511005} + \left(-\frac{3737}{3840} + \frac{101\alpha}{320} \right) \alpha \right) \right) \right) \right) \\
& +t^{1+2\alpha} \alpha^2 \left(\frac{175217821074}{258708615947} + \alpha \left(-\frac{4468054469617}{549755812853} + \alpha \left(\frac{2194833742959}{57869032099} + \alpha \left(-\frac{135239}{1536} + \alpha \left(\frac{551359}{5120} \right. \right. \right. \right. \right. \right. \\
& \left. \left. \left. \left. \left. \left. \right. \right. \right. \right. \right. \right. \right. \\
& +\alpha \left(-\frac{509747}{7680} + \frac{8936108949637\alpha}{549755813493} \right) \right) \right) + t^{1+\alpha} \alpha^3 \left(\frac{2042311253398}{38824134718061} + \alpha \left(-\frac{3343461164686}{4539918978923} \right. \right. \\
& \left. \left. \right. \right. \right. \right. \\
& +\alpha \left(\frac{148067565873822}{35184372088829} + \alpha \left(-\frac{3999146308604}{314146179221} + \alpha \left(\frac{2107347448320}{95609704879} + \alpha \left(-\frac{48121958908668}{2199023255537} \right. \right. \right. \right. \right. \right. \\
& \left. \left. \left. \left. \left. \left. \right. \right. \right. \right. \right. \right. \right. \\
& +\left(\frac{20359290307437}{1759218604423} - \frac{118454052699114\alpha}{46912496118461} \right) \alpha \right) \right) + t\alpha^4 \left(\frac{1}{480} + \alpha \left(-\frac{1}{32} + \alpha \left(\frac{27561091469588}{140737488355343} \right. \right. \right. \right. \right. \right. \\
& \left. \left. \left. \left. \left. \left. \right. \right. \right. \right. \right. \right. \right. \\
& +\alpha \left(-\frac{161}{240} + \alpha \left(\frac{661}{480} + \alpha \left(-\frac{167}{96} + \alpha \left(\frac{186477172070803}{140737488355323} + \left(-\frac{67}{120} + \frac{\alpha}{10} \right) \alpha \right) \right) \right) \right) \right) \left. \right]
\end{aligned}$$

According to Eq. (8), each iteration $u_n(x)$ approaches the solution of Eq. (52), and the approximate solution is expressed as

$$u(x) = \lim_{n \rightarrow \infty} u_n(x) \approx u_3(x).$$

The exact analytical solution for $\alpha = 2$, is given by [35, 36]

$$u(t) = 0.1 - 1.2625t^2 + 0.2104t^3 + 2.6828t^4 - 0.5392t^5 - 2.6563t^6 + 0.6152t^7.$$

The specific case of $\alpha = 2$ shows that the exact solution in Eq. (62) aligns closely with the CTAM solution. Figure 5 (A) illustrates the CTAM solution compared with the exact solution at $\alpha = 2$ and for different α values. Figure 5 (B) presents the absolute error between the 3-rd iteration CTAM solution and the exact solution at $\alpha = 2$. Table 5 provides a comparison between the 3-rd iteration of CTAM, the previous methods in the studies, and the exact solution at various t values for $\alpha = 2$, along with CTAM results for various $\alpha = 1.9$, $\alpha = 1.8$, and $\alpha = 1.7$ showing that the method maintains robust accuracy across different fractional orders, and provide a better error comparing to the result in [36]. The semi-analytical solution approaches the exact solution as the number of iterations grows.

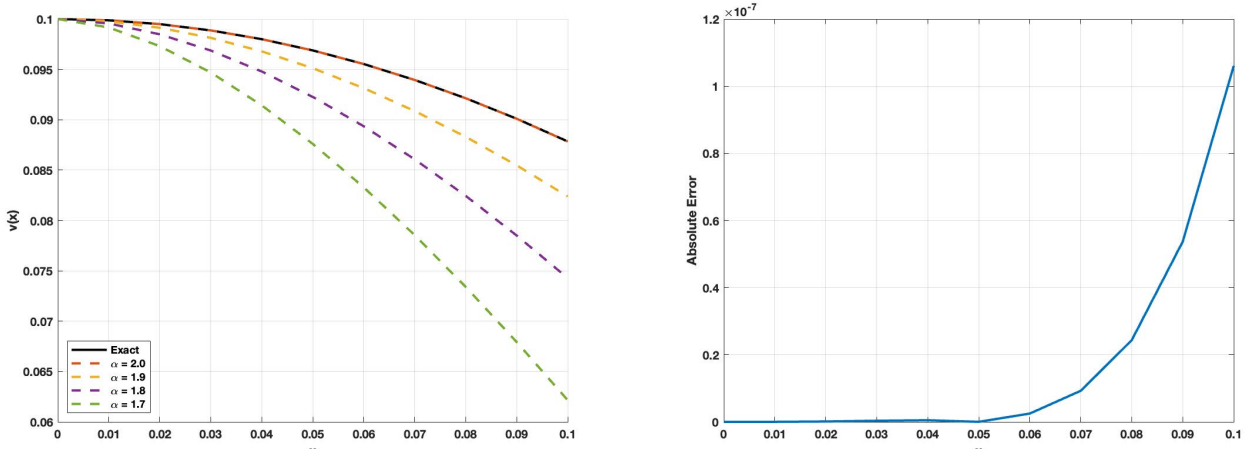


Figure 5: (A) The results of the proposed method in Example 4.5 with 3-rd iteration for different α values and exact solution at $\alpha = 2$. (B) The absolute errors between the proposed method and the exact solution for $\alpha = 2$.

Table 5: A comparison between the 3-rd CTAM solution and the exact solution at $\alpha = 2$ of Example 4.5.

t	u_{Exact}	u_{CTAM} ($\alpha = 2$)	E_{CTAM}	$E_{[36]}$	u_{CTAM} ($\alpha = 1.9$)	u_{CTAM} ($\alpha = 1.8$)	u_{CTAM} ($\alpha = 1.7$)
0.00	0.100000	0.100000	0	0.00000	0.100000	0.100000	0.100000
0.01	0.099874	0.099874	1.646×10^{-11}	7.0821×10^{-7}	0.099767	0.099562	0.099165
0.02	0.099497	0.099497	1.220×10^{-10}	5.4931×10^{-6}	0.099133	0.098484	0.097311
0.03	0.098872	0.098872	3.377×10^{-10}	1.7960×10^{-5}	0.098134	0.096875	0.094692
0.04	0.098000	0.098000	4.859×10^{-10}	4.1211×10^{-5}	0.096791	0.094790	0.091429
0.05	0.096887	0.096887	2.080×10^{-11}	7.7852×10^{-5}	0.095122	0.092271	0.087606
0.06	0.095535	0.095535	2.477×10^{-9}	1.3001×10^{-4}	0.093141	0.089353	0.083290
0.07	0.093949	0.093949	9.269×10^{-9}	1.9934×10^{-4}	0.090863	0.086067	0.078538
0.08	0.092135	0.092135	2.433×10^{-8}	2.8706×10^{-4}	0.088302	0.082441	0.073401
0.09	0.090099	0.090099	5.369×10^{-8}	3.9394×10^{-4}	0.085472	0.078503	0.067926
0.10	0.087847	0.087846	1.060×10^{-7}	5.2036×10^{-4}	0.082386	0.074277	0.062155

Example 4.6. The time-fractional order of the nonlinear Fisher's equation is considered as [37]:

$$\frac{\partial^\alpha u(x,t)}{\partial t^\alpha} = \frac{\partial^2 u(x,t)}{\partial x^2} + u^2(x,t)(1 - u(x,t)), \quad 0 < \alpha \leq 1, x \in \mathbb{I}, t > 0.$$

with the initial condition

$$u(x,0) = \frac{1}{1 + e^{\frac{x}{\sqrt{2}}}}.$$

In this example, the CTAM approach is applied to a time-fractional nonlinear PDE represented by Eq. (63), which is reformulated as

$$\mathcal{L}(u(x,t)) = \frac{\partial^\alpha u(x,t)}{\partial t^\alpha}, \quad \mathcal{N}(u(x,t)) = \frac{\partial^2 u(x,t)}{\partial x^2} + u^2(x,t)(1 - u(x,t)), \quad g(x,t) = 0.$$

The primary issue to address is

$$\mathcal{L}(u_0(x,t)) = 0, \quad u_0(x,0) = \frac{1}{1 + e^{\frac{x}{\sqrt{2}}}}.$$

Which yields the first approximation as

$$u_0(x,t) = \frac{1}{1 + e^{\frac{x}{\sqrt{2}}}}.$$

The following formula can be used to calculate the second iteration

$$\mathcal{L}(u_1(x,t)) + \mathcal{N}(u_0(x,t)) + g(x,t) = 0, \quad u_1(x,0) = \frac{1}{1 + e^{\frac{x}{\sqrt{2}}}}.$$

Consequently, after integration both sides of Eq. (68), results in

$$u_1(x, t) = \frac{2\alpha + e^{\frac{x}{\sqrt{2}}} (2\alpha + t^\alpha)}{2\alpha \left(e^{\frac{x}{\sqrt{2}}} + 1 \right)^2}.$$

The following iteration is then produced by solving

$$\mathcal{L}(u_2(x, t)) + \mathcal{N}(u_1(x, t)) + g(x, t) = 0, \quad u_2(x, 0) = \frac{1}{1 + e^{\frac{x}{\sqrt{2}}}}.$$

By applying the conformable derivative properties 2.1 and integrating both sides of Eq. (70), leads to

$$\begin{aligned} u_2(x, t) = & \frac{1}{96\alpha^4 \left(e^{\frac{x}{\sqrt{2}}} + 1 \right)^6} \left[96\alpha^4 + 12\alpha^2 e^{\frac{5x}{\sqrt{2}}} (8\alpha^2 + t^{2\alpha} + 4\alpha t^\alpha) \right. \\ & + 12\alpha^2 e^{\frac{x}{\sqrt{2}}} (40\alpha^2 - t^{2\alpha} + 4\alpha t^\alpha) + e^{\frac{3x}{\sqrt{2}}} (960\alpha^4 - 8\alpha t^{3\alpha} - 3t^{4\alpha} + 288\alpha^3 t^\alpha) \\ & \left. + 8\alpha e^{2\sqrt{2}x} (60\alpha^3 + 3\alpha t^{2\alpha} + t^{3\alpha} + 24\alpha^2 t^\alpha) + 8\alpha e^{\sqrt{2}x} (120\alpha^3 - 3\alpha t^{2\alpha} - 2t^{3\alpha} + 24\alpha^2 t^\alpha) \right]. \end{aligned}$$

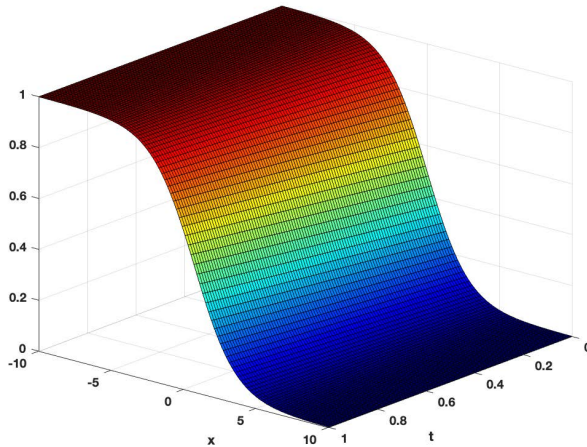
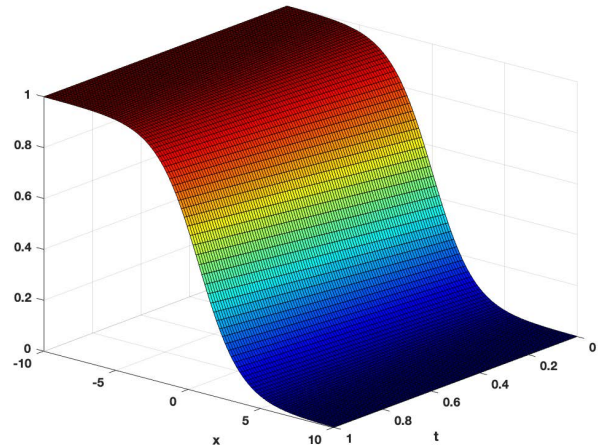
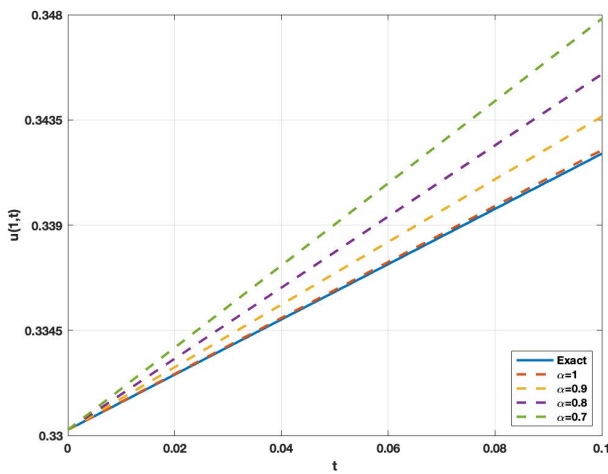
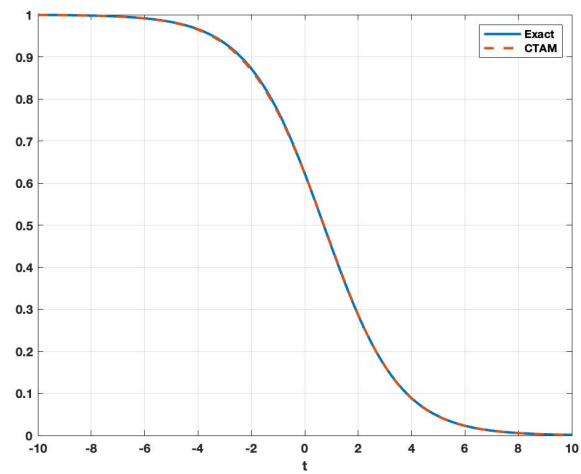
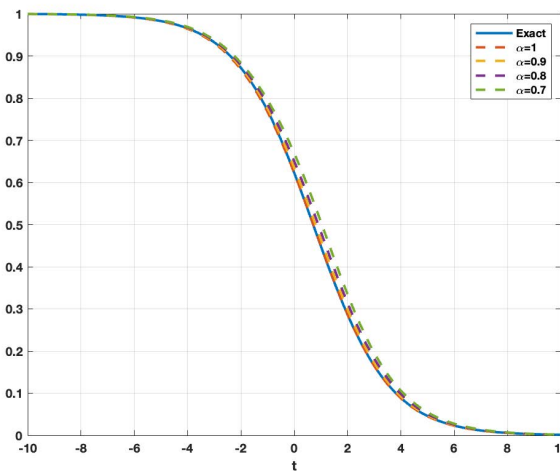
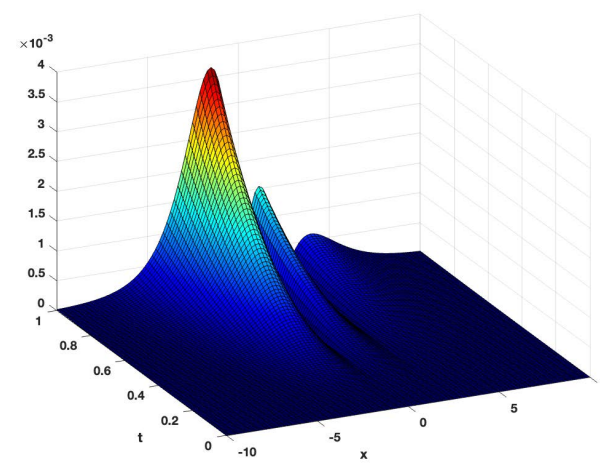
Each iteration of $u_n(x, t)$ is an approximation to the solution of Eq. (63) solution, as shown by Eq. (8). With increasing iterations, the semi-analytical solution converges to the exact solution. Thus, the analytical solution can be approximated by

$$u(x, t) = \lim_{n \rightarrow \infty} u_n(x, t) \approx u_2(x, t).$$

The exact solution for $\alpha = 1$, is given by [37]

$$u(x, t) = \frac{1}{1 + e^{\frac{x-tk}{\sqrt{2}}}}.$$

The analytical results for $\alpha = 1$ demonstrate that the CTAM solution that precisely matches the exact solution in Eq. (63). Notably, the CTAM method is also effective for solving FPDEs. Figure 6 the CTAM results with the exact solution across multiple views. As shown in Subfigures (A) and (B) shows alignment between the analytical and CTAM approximation. Figures 6 (C)-(E) indicate that for fixed values of x and t , CTAM results remain extremely close the exact solution across α values, however the absolute error surface in Figure 6 (F) further confirms the high accuracy of the approach, with minimal error distributed across space and time. Table 6 provides a comparison of the 2-nd iteration CTAM solution with the exact solution for $\alpha = 1$ at $t = 0.1$, under two different parameters, $k = 0.1$ and $k = \sqrt{2}/2$, the CTAM solution demonstrates good agreement with the exact solution, as indicated by the small errors. The results show that the accuracy of the CTAM method improves, and the CTAM solution approaches the exact solution as the number of iterations increases. Demonstrating that the CTAM can produce remarkably accurate solutions in both spatial and temporal dimensions, making it perfectly suited for addressing FPDEs.

(A) Exact solution of $u(x,t)$.(B) CTAM approximate solution of $u(x,t)$.(C) The results of CTAM method for different α values and exact solution at $x = 1$.(D) CTAM solutions compared to the exact solution for different x values when $t = 1$.(E) Comparative of the exact solution at $t = 1$ with various α values.

(F) The absolute errors between the exact solution and CTAM.

Figure 6: A behaves of CTAM analytical solution $u(x,t)$ of Example 4.6 as a function of time t and space x , when $k = \frac{\sqrt{2}}{2}$.

Table 6: A comparison between the 2-nd CTAM solution, and the exact solution at $\alpha = 1$, and $t = 0.1$ of Example 4.6.

x	$k = 0.1$			$k = \frac{\sqrt{2}}{2}$		
	u_{Exact}	u_{CTAM}	E_{CTAM}	u_{Exact}	u_{CTAM}	E_{CTAM}
0	0.501768	0.512497	1.072960×10^{-2}	0.512497	0.512497	4.947900×10^{-8}
1	0.331804	0.341391	9.587100×10^{-3}	0.341390	0.341391	1.543440×10^{-6}
2	0.196685	0.203557	6.871900×10^{-3}	0.203556	0.203557	6.789530×10^{-7}
3	0.107720	0.111915	4.195850×10^{-3}	0.111916	0.111915	3.320900×10^{-7}
4	0.056181	0.058501	2.319580×10^{-3}	0.058501	0.058501	5.629650×10^{-7}
5	0.028513	0.029726	1.213090×10^{-3}	0.029727	0.029726	4.254860×10^{-7}
6	0.014265	0.014881	6.161560×10^{-4}	0.014881	0.014881	2.539760×10^{-7}
7	0.007085	0.007393	3.083360×10^{-4}	0.007393	0.007393	1.371160×10^{-7}
8	0.003506	0.003659	1.531500×10^{-4}	0.003659	0.003659	7.064640×10^{-8}
9	0.001732	0.001808	7.578800×10^{-5}	0.001808	0.001808	3.559070×10^{-8}
10	0.000855	0.000892	3.743570×10^{-5}	0.000892	0.000892	1.773500×10^{-8}

5. Conclusions

The conformable Temimi-Ansari method (CTAM) has been presented as a novel semi-analytical technique for solving FDEs. The efficiency of the method was evaluated through the solution of various examples of nonlinear FDEs, with its effectiveness validated by calculating absolute errors and comparing them to the previous studies. Results were presented using figures and tables using Mathematica and MATLAB to enhance computational speed and accuracy. Owing to CTAM simplicity, adaptability, accuracy, and the smaller error compared to previous studies, the approach demonstrates substantial potential for application to real-world problems that are represented by related classes of FDEs, making it a promising method for future research across a wide range of scientific and engineering applications.

References

- [1] Ahmed El-Sayed, Anas Arafa, I Hanafy, and A Hagag. An approximate study of fisher's equation by using a semi-analytical iterative method. *Progress in Fractional Differentiation and Applications*, **9**(3):397–407, 2023.
- [2] Igor Podlubny. *Fractional differential equations: an introduction to fractional derivatives, fractional differential equations, to methods of their solution and some of their applications*. Elsevier, 1998.
- [3] Shumoua F Alrzqi, Fatimah A Alrawajeh, and Hany N Hassan. An efficient numerical technique for investigating the generalized rosenau–kdv–rlw equation by using the fourier spectral method. *AIMS Mathematics*, **9**(4):8661–8688, 2024.
- [4] Mourad S Semary, Hany N Hassan, and Ahmed G Radwan. Nonlinear fractional order boundary-value problems with multiple solutions. In *Mathematical Techniques of Fractional Order Systems*, pages 37–74. Elsevier, 2018.
- [5] Sad Rida, Anas Arafa, Ahmed Abedl-Rady, and Hamdy Abd-Rahaim. Fractional physical differential equations via natural transform. *Chinese journal of physics*, **55**(4):1569–1575, 2017.
- [6] Xiao-Jun Yang. *General fractional derivatives: theory, methods and applications*. CRC press, 2019.
- [7] K Athira, D Narasimhulu, and Brahmanandam PS. Numerical solutions of timefractional nws and burger's equations using the tarig projected differential transform method (tpdtm). *Contemporary Mathematics*, pages 2907–2928, 2025.
- [8] Abdulrahman BM Alzahrani. Fractional view analysis of coupled whitham-broer-kaup equations arising in shallow water with caputo derivative. *Contemporary Mathematics*, pages 5554–5596, 2024.
- [9] Abir Chaouk and Maher Jneid. Analytic solution for systems of two-dimensional time conformable fractional pdes by using cfrdtm. *International Journal of Mathematics and Mathematical Sciences*, **2019**(1):7869516, 2019.
- [10] Hany N Hassan and Magdy A El-Tawil. Solving cubic and coupled nonlinear schrödinger equations using the homotopy analysis method. *International Journal of Applied Mathematics and Mechanics*, **7**(8):41–64, 2011.
- [11] Mourad S Semary, Hany N Hassan, and Ahmed G Radwan. Modified methods for solving two classes of distributed order linear fractional differential equations. *Applied Mathematics and Computation*, **323**:106–119, 2018.

[12] M Jneid and A Chaouk. The conformable reduced differential transform method for solving newell–whitehead–segel equation with non-integer order. *J. Anal. Appl.*, **18**(1):35–51, 2020.

[13] Farshid Mirzaee and Sahar Alipour. Cubic b-spline approximation for linear stochastic integro-differential equation of fractional order. *Journal of Computational and Applied Mathematics*, **366**:112440, 2020.

[14] Liberty Ebiwareme, Kubugha Wilcox Bunonyo, and Obinna Nwokorie. A novel approximation approach for the analytical solution of the flow of micropolar fluid through a permeable channel. *European Journal of Theoretical and Applied Sciences*, **2**(1):3–17, 2024.

[15] Helmi Temimi and Ali R Ansari. A new iterative technique for solving nonlinear second order multi-point boundary value problems. *Applied Mathematics and Computation*, **218**(4):1457–1466, 2011.

[16] Dmitriy Tverdyi and Roman Parovik. Application of the fractional riccati equation for mathematical modeling of dynamic processes with saturation and memory effect. *Fractal and Fractional*, **6**(3):163, 2022.

[17] Mohammad Izadi. Approximate solutions for solving fractional-order painlevé equations. *Contemporary Mathematics*, pages 12–24, 2019.

[18] Craig A Tracy and Harold Widom. Random unitary matrices, permutations and painlevé. *Communications in mathematical physics*, **207**:665–685, 1999.

[19] Ruqiong Qin and Chunyi Duan. The principle and applications of bernoulli equation. In *Journal of Physics: Conference Series*, volume 916, page 012038. IOP Publishing, 2017.

[20] Vrani Ibarra-Junquera and Haret C Rosu. Pi-controlled bioreactor as a generalized liénard system. *Computers & chemical engineering*, **31**(3):136–141, 2007.

[21] Carlo Cattani and Aleksey Kudreyko. Mutiscale analysis of the fisher equation. In *International conference on computational science and its applications*, pages 1171–1180. Springer, 2008.

[22] José Canosa. On a nonlinear diffusion equation describing population growth. *IBM Journal of Research and Development*, **17**(4):307–313, 1973.

[23] Maher Jneid. New conformable fractional hpt for solving systems of linear and nonlinear conformable fractional pdes. *Italian J. Pure Appl. Math.*, **48**:1242–1253, 2022.

[24] Feng Gao and Chunmei Chi. Improvement on conformable fractional derivative and its applications in fractional differential equations. *Journal of Function Spaces*, **2020**(1):5852414, 2020.

[25] Maher Jneid and Abdallah El Chakik. Analytical solution for some systems of nonlinear conformable fractional differential equations. *Far East J. Math. Sci.*, **109**(2):243–259, 2018.

[26] Roshdi Khalil, Mohammed Al Horani, Abdelrahman Yousef, and Mohammad Sababheh. A new definition of fractional derivative. *Journal of computational and applied mathematics*, **264**:65–70, 2014.

[27] Xiao-Jun Yang, Dumitru Baleanu, and Hari M Srivastava. *Local fractional integral transforms and their applications*. Academic Press, 2015.

[28] Thabet Abdeljawad. On conformable fractional calculus. *Journal of computational and Applied Mathematics*, **279**:57–66, 2015.

[29] Helmi Temimi and Ali R Ansari. A semi-analytical iterative technique for solving nonlinear problems. *Computers & Mathematics with Applications*, **61**(2):203–210, 2011.

[30] Anas AM Arafa, Ahmed MA El-Sayed, and Ahmed M SH. Hagag. A fractional temimiansari method (ftam) with convergence analysis for solving physical equations. *Mathematical Methods in the Applied Sciences*, **44**(8):6612–6629, 2021.

[31] Aisha F Fareed, Menna TM Elbarawy, and Mourad S Semary. Fractional discrete temimi–ansari method with singular and nonsingular operators: applications to electrical circuits. *Advances in Continuous and Discrete Models*, **2023**(1):5, 2023.

[32] Aisha F Fareed, Mourad S Semary, and Hany N Hassan. An approximate solution of fractional order riccati equations based on controlled picard's method with atangana–baleanu fractional derivative. *Alexandria Engineering Journal*, **61**(5):3673–3678, 2022.

[33] Esmail Hesameddini and Amir Peyrovi. The use of variational iteration method and homotopy perturbation method for painlevé equation i. *Applied Mathematical Sciences*, **3**(37–40):1861–1871, 2009.

[34] MD Johansyah, AK Supriatna, E Rusyaman, and J Saputra. Bernoulli fractional differential equation solution using adomian decomposition method. In *IOP Conference Series: Materials Science and Engineering*, volume 1115, page 012015. IOP Publishing, 2021.

[35] S Nourazar and A Mirzabeigy. Approximate solution for nonlinear duffing oscillator with damping effect using the modified differential transform method. *Scientia Iranica*, **20**(2):364–368, 2013.

[36] Harendra Singh and Hari Mohan Srivastava. Numerical investigation of the fractionalorder liénard and duffing equations arising in oscillating circuit theory. *Frontiers in Physics*, **8**:120, 2020.

[37] Mehdi Bastani and Davod Khojasteh Salkuyeh. A highly accurate method to solve fisher's equation. *Pramana*, **78**:335–346, 2012.